Science of the Total Environment 647 (2019) 1266–1280

Contents lists available at ScienceDirect

Science of the Total Environment

journal homepage: www.elsevier.com/locate/scitotenv

Improving estimates of built-up area from night time light across globally distributed cities through hierarchical modeling

Zutao Ouyang [a,*], Meimei Lin [b], Jiquan Chen [a], Peilei Fan [c], Song S. Qian [d], Hogeun Park [a]

[a] Center for Global Change and Earth Observations (CGCEO), Michigan State University, East Lansing, MI 48823, USA
[b] Department of Geology and Geography, Georgia Southern University, Savannah, GA 31419, USA
[c] School of Planning, Design, and Construction and Center for Global Change and Earth Observations (CGCEO), Michigan State University, East Lansing, MI 48823, USA
[d] Department of Environmental Sciences, University of Toledo, Toledo, OH 48606, USA

HIGHLIGHTS

- Improved estimates of built-up area were achieved from nighttime light.
- A hierarchical hockey-stick model was used to consider local settings of cities.
- Bayesian framework provides a prior model for future updating with new data.
- The influence of local urban settings on estimating built-up area was investigated.

GRAPHICAL ABSTRACT

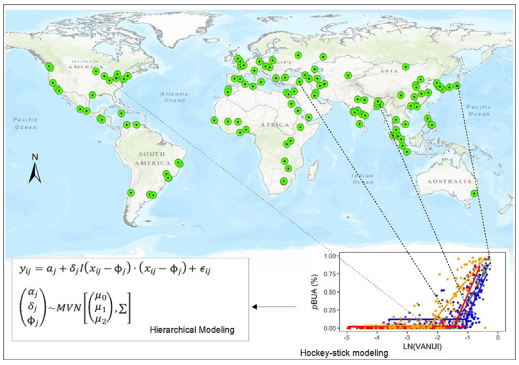

ARTICLE INFO

Article history:
Received 22 June 2018
Received in revised form 30 July 2018
Accepted 2 August 2018
Available online 04 August 2018

Editor: Jay Gan

Keywords:
Bayesian
Hierarchical model
Urban land
DMSP-OLS
MODIS
Human settlement

ABSTRACT

Built-up area has become an important indicator for studying urban environments, but mapping built-up area at the regional/global scale remains challenging due to the complexity of impervious surface features. Nighttime light data (NTL) is one of the major remote sensing data sources for regional/global built-up or impervious surface mapping. A single regression relationship between fractional built-up/impervious area and NTL or various indices derived based on NTL and vegetation index (e.g., NDVI) data had been established in many previous studies. However, due to the varying geographical, climatic, and socio-economic characteristics of cities, the same regression relationship may vary significantly across cities. In this study, we examined the regression relationship between percentage of built-up area (*p*BUA) and vegetation adjusted nighttime light urban index (VANUI) for 120 randomly selected cities around the world with a hierarchical hockey-stick regression model. We found that there is a substantial variability in the slope (0.658 ± 0.318), the threshold VANUI (-1.92 ± 0.769, log scale) after which the linear relationship holds, and the coefficient of determination R^2 (0.71 ± 0.14) among globally distributed cities. A small proportion of this substantial variability can be attributed to socio-economic status (e.g., total population, GDP per capita) and landscape structures (e.g., compactness and fragmentation). Due to these variations, our hierarchical model or no-pooling model (i.e., fit each city individually) can significantly improve model prediction accuracy (17% in terms of root mean squared error) over a complete-pooling model. We, however, recommend hierarchical models as they can provide meaningful priors for future modeling under a Bayesian framework, and achieve higher prediction accuracy than no-pooling models when sample size is small.

* Corresponding author at: 1405 S. Harrison, East Lansing, MI 48823, USA.
E-mail address: yangzuta@msu.edu (Z. Ouyang).

https://doi.org/10.1016/j.scitotenv.2018.08.015
0048-9697/

1. Introduction

The United Nations has projected that two thirds of the global population will live in cities by 2050. Urban sprawl has led to increasing environmental degradation of cities and their adjacent areas, such as air pollution and urban heat islands, as well as an alarmingly increased social disparity in income, housing, and access to urban amenities such as public green spaces, education and health care (Chen et al., 2016; Estoque et al., 2017; Fan et al., 2017; Nassauer et al., 2014; Park et al., 2017). Accurate delineation of urban land plays a fundamental role in urban studies, such as quantifying urban sprawl, performing environmental assessments, planning, etc. (Alberti, 2005; Wu, 2014). Hence, timely mapping of urban lands at regional and global scales has considerable significance for policy makers to make appropriate urban planning and policy decisions (Elvidge et al., 2007; Mertes et al., 2015; Pesaresi et al., 2013).

Satellite images that record nighttime light (NTL) from the Defense Meteorological Satellite Program's Operational Linescan System (DMSP-OLS) are one of the main data sources for mapping urban land in terms of built-up area or impervious surface area distribution, especially at regional and global scales (Elvidge et al., 2007; Li and Zhou, 2017; Zhang and Seto, 2011). Earlier studies have used the threshold-based approach to extract regional distributions of built-up area (Liu and Leung, 2015; Xiao et al., 2014), but the results carried high levels of uncertainty because no single optimal threshold could be identified for delineating built-up area from other land cover types across the complex urban landscapes (Zhou et al., 2015b). More critically, the original DMSP-OLS data has a spatial resolution of ~2.7 km and was resampled to 1 km with a digital number (DN) of 0–63, indicating potential concerns resulting from mixed-pixels and saturation of luminosity. These potential problems would propagate the blooming effect (Li and Zhou, 2017) and lead to overestimation of urban land, especially in rapid transitional regions of urban-suburban complexes. Consequently, NTL alone cannot provide accurate built-up area estimates. To overcome these issues, several efforts have been made to integrate DMSP-OLS with the Moderate Resolution Imaging Spectroradiometer (MODIS), another source of coarse spatial resolution data (Angel et al., 2016; Guo et al., 2017, 2015; Lu and Weng, 2006; Zhang et al., 2013), to improve the accuracy and performance of built-up area mapping from NTL.

MODIS vegetation index products can help distinguish built-up area from other non-vegetation covers (e.g., bare land and water) in addition to reducing the mixed-pixel problem (e.g., 250–1000 m spatial resolutions) and resolving the data-saturation issue (e.g., using its 16-bit data depth) that exists in DMSP-OLS NTL. Numerous studies have demonstrated the effectiveness of integrating DMSP-OLS and MODIS (or other similar products that provide vegetation information) in improving the performance of built-up/impervious area mapping at regional and global scales (Angel et al., 2016; Guo et al., 2017, 2015; Li and Zhou, 2017; Lu and Weng, 2006; Zhang et al., 2013). Lu and Weng (2006), for example, pioneered a human settlement index (HSI) based on DMSP-OLS and MODIS normalized difference vegetation index (NDVI) data to estimate the settlement areas in south and east China. Later, similar indices combining NTL data and other vegetation indices (e.g., MODIS NDVI, or enhanced vegetation index-EVI, and SPOT NDVI, etc.) were also proposed to improve the mapping performance (Cao et al., 2009; Guo et al., 2017, 2015; Zhang et al., 2013; Zhuo et al., 2015).

The vegetation adjusted nighttime light urban index (VANUI) was derived from the normalized DMSP-OLS NTL and MODIS NDVI data, and was suggested as a better index than HSI in correlation to the built environment (Zhang et al., 2013). Following this school of thought, Zhuo et al. (2015) used the enhanced vegetation index (EVI) instead of NDVI, and developed an EVI-adjusted nighttime light index (EANTLI) to reduce the data saturation problem within the DMSP-OLS NTL data. A large-scale impervious surface index (LISI) was also developed by combining higher resolution (750 m) NTL data from DMSP-OSL (e.g., Visible Infrared Imaging Radiometer Suite's Day/Night Band, VIIRS-DNB) with MODIS NDVI (Guo et al., 2015) for the same purpose. Guo et al. (2017) also integrated the normalized impervious surface index (NISI) with DMSP-OLS NTL and MODIS NDVI in delineating impervious area.

The performances of mapping urban landscapes depend on the strength of the linear relationships between impervious/built-up area and the NTL-based index (e.g., HSI, VANUI, EANTLI, LISI, or NISI) at the pixel level. Linear regressions have been used to predict impervious/built-up area from the aforementioned indices at the city and regional level (Guo et al., 2017, 2015; Lu and Weng, 2006). Here a common pitfall in previous studies is that the regression models were trained by a pooled random sample from multiple cities by assuming that a single, universal regression relationship between a preferred index and impervious/built-up area exists. This approach ignores the potentially different relationships among cities. In reality, the empirical relationships may vary significantly by city because of unique local settings. Lighting systems between developed and developing countries may differ significantly because their economic status may prevent or promote installations of lighting in built-up environments; and national/regional policies and cultures may yield different usages of nighttime lights. For instance, Germany does not usually light its autobahns, but the U.S. illuminates its city roads and highways intensively (Kyba et al., 2014). Consequently, this one-model-fits-all strategy in mapping impervious/built-up area can potentially produce very different results when applied across globally/regionally distributed cities. Altogether, the same empirical relationship might perform better for some cities than for others. Ignoring the potential differences among cities will lead to substantial over- or under-estimations of impervious/built-up area both locally and regionally. While some studies have already showed that the relationship between urban land and NTL (or an index based on NTL) differs dramatically across cities even within a single country (Gao et al., 2015), and across countries (Liu and Leung, 2015; Zhou et al., 2015a), there has been no single study that has specifically examined these variations yet (Bennett and Smith, 2017).

Clearly, it is crucial to include quantitative information on inter-city differences across the global range of socioeconomic status, climatic conditions, geographic settings, etc., as well as intra-city characteristics (e.g., landscape structure) in model development. As built-up and impervious area are similar quantities that are widely used for urban land and human settlement mapping, we selected built-up area (simply because we have training data in the form of built-up area), to demonstrate the needs of hierarchical modeling to improve the accuracy of estimates from NTL. Specifically, we set our study objectives to: 1) estimate the magnitude of the variation of the relationship between built-up area and a NTL-based index among globally distributed cities; 2) explore the potential contributions of within-city characteristics to the variation; and more importantly, 3) improve the built-up area estimates through Bayesian hierarchical modeling (BHM) through considering local settings. In pursuing these objectives, we hypothesize that the same regression model for predicting built-up area from NTL-based indices will be statistically different among cities, but incorporating these differences into modeling will enhance the performance in delineating built-up area.

2. Methods and materials

2.1. The global sample of cities

We focused on the global variation of the relationships between the percentage of built-up area (*p*BUA) and NTL-based indices. In this study, we used the global sample of 120 cities from Angel et al. (2005) (Fig. 1). These 120 cities are a stratified random sample drawn from 3943 distinct metropolitan areas that had populations in excess of 100,000 in 2000. Angel et al. (2005) selected these cities by considering three important stratification characteristics: (1) the geographical region in which the city is located; (2) the city size; and (3) the level of economic

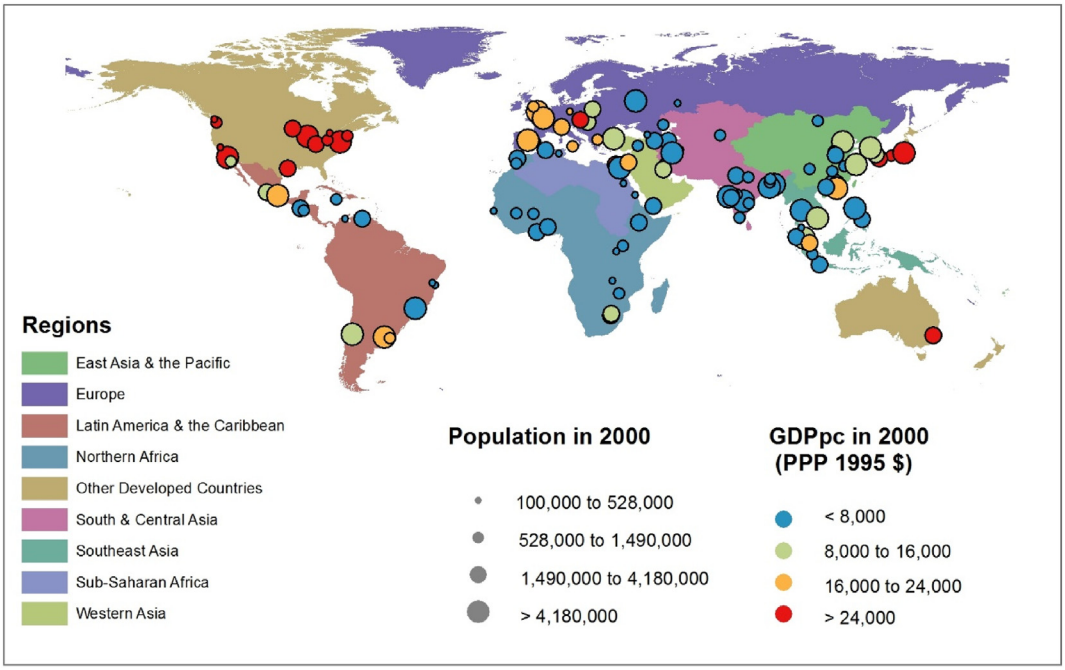

Fig. 1. The global distribution of the 120 cities by region, population size, and GDP per capita (GDPpc) used in this study. These cities were the same ones as those in Angel et al. (2005). We updated the database to show the GDPpc (adjusted PPP in 1995) at the city level for 2000. Note that regions are defined by grouping countries and Russia is classified as a European country.

development of the country in which the city is located, measured by Gross National Product per capita (GNPpc). Angel et al. (2005) provided a detailed rationale for the selection process.

2.2. Data

Among the widely used NTL indices, we used VANUI in this study to establish its relationship with *p*BUA because of its easy computation and high correlation with *p*BUA. A global VANUI image in 2000 was produced following Zhang et al. (2013) using the composite F14 DMSP/OLS image, and the 8-day 500-m MODIS NDVI products:

$$\mathrm{VANUI} = (1 - \mathrm{NDVI}) \cdot \mathrm{NTL} \quad (1)$$

where NDVI is the maximum NDVI extracted from the 500-m MODIS NDVI composites, and NTL is the normalized NTL. In this study, we did not use the mean annual NDVI value (e.g., Zhang and Seto (2011)) because the maximum NDVI can better reflect the distributions of green vegetation and eliminate the effects caused by cloud and shadow contamination that are common in the time-series MODIS NDVI data (Guo et al., 2017). The *p*BUA data at each 1000-m resolution pixel were calculated based on built-up area classification from Landsat images. Angel et al. (2005) produced the 30-m land cover maps for all of the 120 cities based on Landsat images by classifying a city into three classes: urban built-up land, water, and other lands. Each city was divided into 1 × 1 km grids that geographically match the pixels in the VANUI layers; *p*BUA of each grid was computed based on the 30-m urban built-up maps. All 1 × 1 km pixels with VANUI of >0 were retained as our data sample for modeling, yielding a total of 541,696 pixels at 1 km resolution from the 120 cities for Bayesian hierarchical modeling (Section 2.5).

To identify the significant socioeconomic and geophysical factors that might affect the city-level *p*BUA-VANUI relationships, we collected other ancillary data at the city level (Table 1). These data include variables representing climatic conditions and biomes information (i.e., precipitation, temperate, and elevation), geographical locations (i.e., latitude, longitude), landscape structures (i.e., BUA, BUA density, openness, proximity, and cohesion), and socioeconomic conditions (i.e., populations, GDP per capita – GDPpc). Openness, proximity, and cohesion are landscape metrics describing the landscape structure of a city.

Table 1
Socioeconomic and bio-geophysical variables collected for each of the 120 cities for their influences in *p*BUA-VANUI relationships through hierarchical modeling. GDPpc were converted from nominal value to PPP 1995 $ value to ensure their compatibility among different cities.

Name	Description	Unit	Category
Population	The total population	X 1000	Socioeconomic conditions
GDPpc	GDP per capita	PPP 1995 $	Socioeconomic conditions
BUA	The built-up area	m^2	Landscape structures
BUA density	The built-up area per person	m^2/person	Landscape structures
Openness	Fragmentation	1	Landscape structures
Proximity	An index to present compactness	1	Landscape structures
Cohesion	An index to present compactness	1	Landscape structures
Precipitation	Total annual precipitation	mm	Climatic and biome zones
Temperature	Annual mean air temperature	C	Climatic and biome zones
Elevation	Mean elevation above sea	m	Climatic and biome zones
Latitude	Latitude	Degree	Geographic locations
Longitude	Longitude	Degree	Geographic locations

Openness measures fragmentation attributes of cities, which is the average percentage of non-ISA area in a 1-km diameter circle surrounding each pixel in the city (Angel et al., 2005; Burchfield et al., 2006). Proximity and cohesion are two correlated indices that describe the compactness of a city. Proximity is the ratio of the average straight-line distance of all points in an equal area circle to city hall to the average straight-line distance of all points in the urban extent to city hall; cohesion is the ratio of the average straight-line distance of all points to all other points in an equal area circle to the average straight-line distance of all points to all other points in the urban extent (Angel et al., 2016). The equal area circle is a circle with equal land area to the urban ISA extent that is centered at city hall. Population and GDPpc were collected from the Atlas of Urban Expansion (http://www.atlasofurbanexpansion.org/), the Bureaus of National Statistical Office, and the World Data Atlas (https://knoema.com). While we successfully collected population data for all 120 cities, we did not find GDPpc data for a few cities. For these cities (e.g., Ansan and Chonan in South Korea, Medan in Indonesia, Kampala in Uganda, and Tacoma in the United States of America), we instead utilized provincial/state statistics of GDPpc as approximated values. Precipitation (annual sum) and temperature (annual mean) were collected from cities' climatic stations. Elevation was derived from the SRTM 30 m DEM (https://www2.jpl.nasa.gov/srtm/).

2.3. Exploratory analysis

Previous studies have suggested that a linear regression relationship exists between a NTL-based index (e.g., HSI and VANUI) and the percentage of impervious/built-up area (Guo et al., 2017; Lu and Weng, 2006; Zhang and Seto, 2011). A log transformation of the index would further strengthen the empirical models (Lu and Weng, 2006), because the distributions of these indices are slightly skewed. Therefore, natural log transformed VANUI was applied in this study. We fitted Loess lines (Cleveland, 1993) to data points from individual cities to explore the potential relationships (Fig. 2). Loess analysis suggested that a hockey-stick model (e.g., piecewise/segmented linear model) (Qian, 2016) best fit the data. The hockey-stick model is also conceptually reasonable because pixels that include negligible built-up area might be illuminated by adjacent urban light due to the blooming effects, suggesting that a strong *p*BUA-VANUI relationship may only appear above a threshold of VANUI.

2.4. Data grouping

Data grouping is different and independent from stratified sampling of cities. The stratification for city selection conducted by Angel et al.

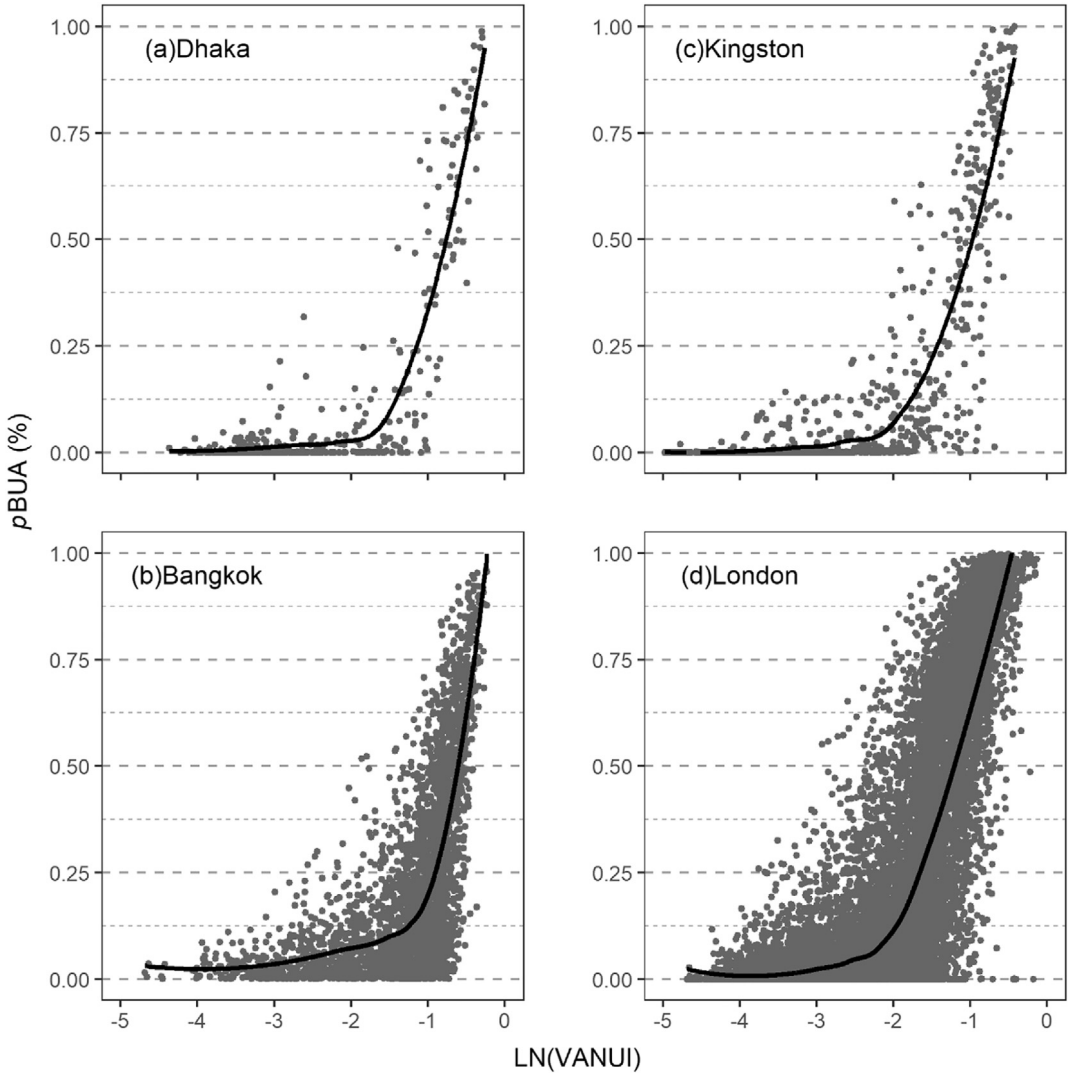

Fig. 2. Exploratory Loess analysis shows that a hockey-stick model can properly describe the changes in the percentage of impervious surface area (*p*BUA) with vegetation adjusted nighttime light urban index (VANUI). Only four selected cities were presented in this figure for demonstration purposes.

(2005) was to ensure that the 120 cities were representative of all globally distributed cities. Because our emphasis is on the unique setting of each city, we grouped our data (541,696 pixels) by cities to be consistent with our model structure (see Section 2.5, Hierarchical Modeling), i.e., each pixel is labeled to belong to the city where it was sampled. Therefore, we have in total 120 groups (cities).

2.5. Hierarchical modeling

Our exploratory analyses suggest that a simple linear regression is inadequate to model the relationship between *p*BUA and VANUI. This deficiency also appeared in previous studies that applied a simple linear regression. For example, Lu and Weng (2006) (i.e., the residuals, Fig. 9) found two distinct values of the regression slope, which is in contrast to those (i.e., Fig. 1) of Qian (2014). A similar phenomenon was also apparent in Figure 5 of Guo et al. (2017). Based on our exploratory analyses and the residual assessments of the above referenced papers, a hockey-stick model seems more appropriate, which can be expressed as:

$$y_i = \alpha + [\beta + \delta \cdot I(x_i - \phi)](x_i - \phi) + \varepsilon \tag{2}$$

where α is the intercept of the first line segment, β is the slope of the first line segment, δ is the difference in slope between the first and second line segment, ϕ is the threshold value where the line slope changes, ε is the model residuals, and I is a function defined as:

$$\mathrm{I}(z) = \begin{cases} 0, & z \le 0 \\ 1, & z > 0 \end{cases} \tag{3}$$

*p*BUA is almost invariable to VANUI when it is less than ϕ (Fig. 2). Even though there is a small rate of change of *p*BUA with VANUI when it is $<\phi$, such a level of change is of no practical importance. Hence, we forced β to zero (i.e., there exists no linear relationship between *p*BUA and VANUI when VANUI is less than ϕ). As a result, our model is simplified as:

$$y_i = \alpha + \delta \cdot I(x_i - \phi) \cdot (x_i - \phi) + \varepsilon \tag{4}$$

An advantage of this hockey-stick model is its generalization for covering all previous models. For example, the hockey-stick model (Eq. (2)) is the same as a linear model when $\delta = 0$ or ϕ approaches the minimum or maximum VANUI.

Previous studies have assumed that the same set of model coefficients could be applied for a group of cities (Guo et al., 2017; Lu and Weng, 2006). This approach, also known as "complete pooling", implies that data from different cities are true replicates. As argued in previous text, however, the *p*BUA-VANUI relationship may vary because many factors affecting the relationship may exist and can operate at different spatial scales (Qian et al., 2010; Yun and Qian, 2015). In addition, data pixels from different cities should not be treated as true replicates because they are not necessarily governed by the same processes. On the other hand, if we treat all cities independently (no-pooling method), there would be an oversight that *p*BUA and VANUI data from one city may partially represent another. For example, two pixels with the same VANUI values from two different cities are very likely to have similar *p*BUA. Furthermore, no-pooling might have limited statistical power for groups with a small sample size (Shelton et al., 2012; Yun and Qian, 2015). These weaknesses associated with the complete-pooling, or no-pooling models, can be overcome by applying Bayesian hierarchical modeling (BHM) (Gelman and Hill, 2007). A multilevel/hierarchical model treats samples within a group (e.g., city) as replicates and adjusts the estimated model coefficients based on data from a specific group by shrinking them towards the overall mean of the same coefficients for all groups. In BHM, the overall means are regarded as a common prior for all cities. This adjustment is commonly known as shrinkage estimation, with a shrinkage estimator being superior (in terms of a model's predictive accuracy) to its maximum likelihood (unshrunk) counterpart (Qian et al., 2015a, 2015b).

A complete-pooling model uses all pixel samples from all cities in Eq. (4), while a no-pooling model will use data from each city independently resulting in a city-specific model. In the hierarchical model, model coefficients are city-specific, and their shared characteristics are reflected by a common prior imposed on these coefficients:

$$y_{ij} = a_j + \delta_j I\left(x_{ij} - \phi_j\right) \cdot \left(x_{ij} - \phi_j\right) + \epsilon_{ij} \tag{5a}$$

$$\begin{pmatrix} \alpha_j \\ \delta_j \\ \phi_j \end{pmatrix} \sim MVN\left[\begin{pmatrix} \mu_0 \\ \mu_1 \\ \mu_2 \end{pmatrix}, \sum\right] \tag{5b}$$

where *ij* represents the *i*th pixel from the *j*th city. The city-specific coefficients a_j, δ_j, and ϕ_j were assumed to share a common prior distribution, i.e., a multi-variate normal (MVN) distribution with mean of $[\mu_0, \mu_1, \mu_2]$, and a variance-covariance matrix $\sum$, where the covariance matrix is formed by the variance σ_0, σ_1, and σ_2, and the paired correlations between a_j, δ_j, and ϕ_j.

This model (Eqs. (5a), (5b)) accounts for within-group (i.e., pixels within a city) and among-group variations simultaneously, which allows us to investigate the global variations of the *p*BUA-VANUI relationships. With this hierarchical structure, pixels within a city are assumed as true replicates and the empirical coefficients are city-specific. These city-specific coefficients are further assumed to be exchangeable and share the same prior distribution (Eq. (5b)). The model was fitted using the Markov Chain Monte Carlo (MCMC) simulation in R package RStan using a Bayesian approach. Computed sources from the High Performance Computing Center (HPCC) at Michigan State University were used to run 20 parallel MCMC chains each at 10,000 iterations with 5000 for warming. The Gelman-Rubin diagnostic processes (Gelman and Rubin, 1992) and visual check of parallel chains were performed to ensure convergence of parameters and the chains.

2.6. Quantifying the differences among cities

We did not include any group-level predictors for a_j, δ_j, and ϕ_j in model (Eqs. (5a), (5b)). Instead, we only applied the exchangeability assumption (i.e., a_j, δ_j, and ϕ_j vary around the mean of μ_0, μ_1, and μ_2). This is a reasonable way to express our ignorance about the variation of city-specific model coefficients: the coefficients vary by city but are otherwise uncertain (because we do not know a priori whether the slope δ_j in one city is higher/lower than another city and why). Therefore, we performed a post-model analysis to explore the driving forces on variation of city-specific model coefficients.

Because the slope of the first segment was forced to zero and the intercept (a_j) only represents the background noise of *p*BUA in our hockey-stick models, we focused on the discussion of δ_j as the slope of the second segment (hence why we did not report the a_j for post-analysis). Meanwhile, we were also interested in the performances of the same hockey-stick model among cities. In this regard, we used the widely used r-square (R_j^2) as the goodness of fit criteria in assessing model performance. Since BHM does not provide R^2 estimation directly, we computed R^2 by: (1) predicting *p*BUA based on the posterior distribution of a_j, δ_j, and ϕ_j, and (2) comparing predicted values with observed *p*BUA.

The relationship between city-specific model coefficients (δ_j and ϕ_j) and the city-specific R_j^2, and the city level variables (Table 1) were investigated through correlation analysis and random forests, aiming to find any possible regulators for among-city variation in the *p*BUA-VANUI relationships. Random forests were applied because of its capability in capturing non-linear features through both regression and classification (Bento et al., 2013). We checked the changes in mean accuracy (out-of-bag errors) and Gini (node impurity of variables) to identify the most

important variables in the random forests. More specifically, we computed the mean decreases in the accuracy and Gini when the variable was randomly permuted. Population, GDPpc, BUA, and BUA density appeared log-normally distributed, so they were log-transformed.

2.7. Model comparisons

We first compared the predictive accuracy among different model structures for all 120 cities. The no-pooling model (e.g., Eq. (4) applied to samples from each city separately) and the complete-pooling model (e.g., Eq. (4) applied to the pooled sample from all cities) were also developed with the Bayesian approach for the purpose of comparison. We first compared the cross-validated RMSE (root mean square error) among the three model structures, with half of the total dataset to train the model and the other half for validation. While RMSE has been widely used as a conventional residual-based model assessment, it is not appropriate for the comparisons of Bayesian models, especially for BHM (Qian et al., 2015b). We therefore also compared the Watanabe-Akaike Information Criterion (WAIC) (Watanabe, 2010), which is a fully Bayesian implementation of information theoretical methods in assessing a model's predictive accuracy (Gelman et al., 2014). WAIC has also been regarded as a measure of deviance and is proportional to the mean squared error when the response variable is normal (Qian et al., 2015b). Because of the computational intensity required for calculating WAIC, the current implementation of WAIC in R cannot process data of the size of our study. As a result, WAIC was calculated using a subset of cities. We selected cities in China and the United States (because the two countries have the most cities in our city sample) as demonstrative cases. We made the model comparisons using WAIC among the BHM, the no-pooling model, and the complete-pooling model for these two sets of cities. To reduce the overwhelming computation time, we further reduced the data size by randomly

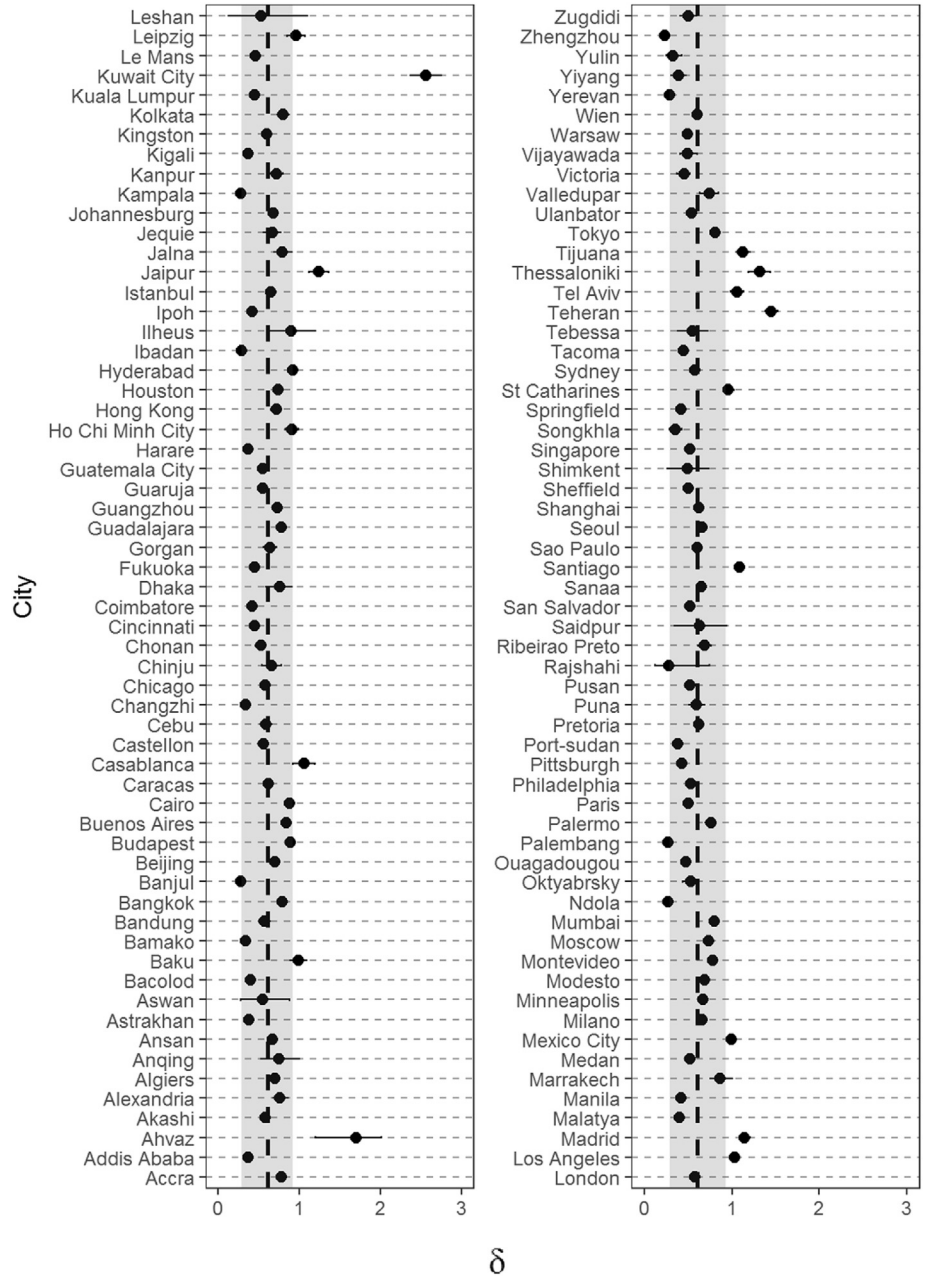

Fig. 3. The estimated mean (black dots) and the 90% credible intervals (black solid horizontal lines) of the slope δ for the second segment of the hockey-stick model in 120 cities based on Bayesian hierarchical model (BHM). The shaded areas are the overall mean (black dotted vertical line) $\pm$ standard deviation (i.e., $\mu_1 \pm \sigma_1$, where μ_1 and σ_1 are the hyper parameters describing the distribution of δ, see Section 2.5 for more details).

sampling up to 50 pixels per city (i.e., a small sample) and up to 800 pixels per city (i.e., a large sample) for these two sets of cities.

3. Results

3.1. The variations among cities

While the same hockey-stick model was successfully developed for each city, the model coefficients varied greatly among the 120 cities. The slope (δ) varied from a low value of 0.23 for Zhengzhou, China, to a high value of 2.56 for Kuwait City, Kuwait (Fig. 3); the VANUI threshold (ϕ) was the lowest for Ibadan, Nigeria (-4.73) and the highest (-0.30) for Kuwait City, Kuwait (Fig. 4). Most of the cities had a very narrow 90% credible interval for both the slope and the threshold, suggesting a precise estimate. However, a few cities had larger uncertainties associated with the mean estimates, including Ahvaz, Anqing, Aswan, Casablanca, Chinju, Dhaka, Leshan, Marrakech, Leipzig, Kuwait City, Rajshahi, Saidpur, Shimkent, Tebessa, etc. (Figs. 3 and 4). The slope and the VANUI threshold were statistically different between many pairs of cities even when they were from the same region or country; for example, Zhengzhou and Yiyang from China, and Los Angeles and Minneapolis from the United States. Statistical difference here is defined as the 90% credible intervals of two cities that do not overlap, which corresponds to $p = 0.1$. The slopes of most cities were inside of one standard deviation of the overall mean, with a few exceptions (Ahvaz, Jaipur, Los Angeles, Madrid, Teheran, Tel Aviv, Thessaloniki, and Tijuana). These cities are either located in the deserts & xeric shrublands or in the Mediterranean forests, woodlands and scrub biome where climate is dry, which may relate to the small ranges of NDVI due to sparse vegetation. The VANUI threshold seems more variable than the slope, with more cities falling outside the one standard deviation of the mean. These cities with the lowest VANUI threshold were

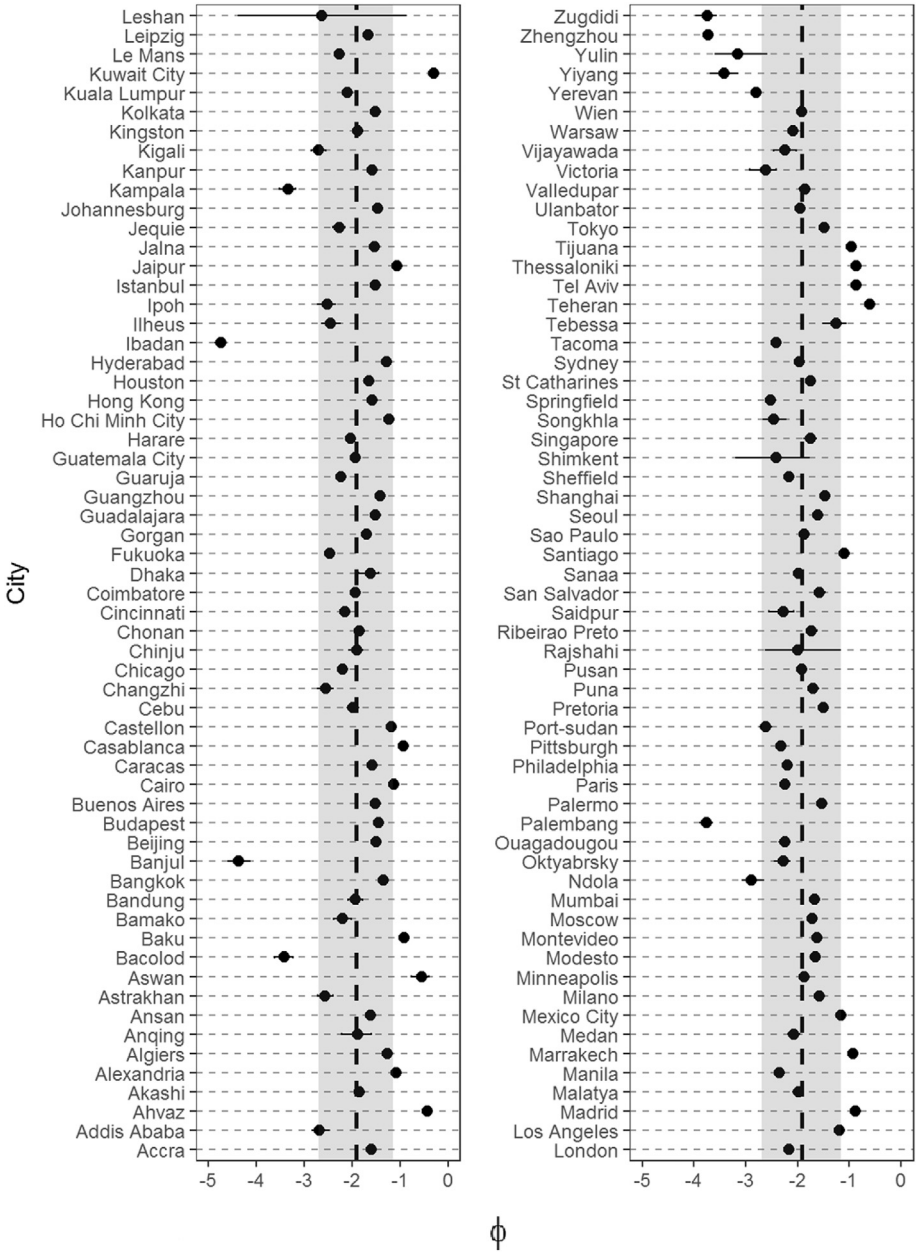

Fig. 4. The estimated mean (black dots) and the 90% credible intervals (black solid horizontal lines) of the VANUI threshold (ϕ) for the hockey-tick model based on Bayesian hierarchical model (BHM). The shaded areas are the overall mean (black dotted vertical line) $\pm$ standard deviation (i.e., $\mu_2 \pm \sigma_2$, where μ_2 and σ_2 are the hyper parameters describing the distribution of δ, see Section 2.5 for more details).

from low- or lower-middle-income countries/regions in Africa (e.g., Banjul of Gambia, Ibadan of Nigeria, Kampala of Uganda, and Marrakech of Morocco) and Asia (e.g., Bacolod of Philippines, Palembang of Indonesia, and Zhengzhou, Yulin, Yiyang that located in provinces of China with laggard economy). Cities with the highest VAUNI thresholds were observed from high-income countries (e.g., Kuwait City, Madrid, and Los Angeles), but could also be found in populous cities from lower-and upper-middle-income countries (e.g., Ahvaz, Aswan, Teheran etc.). In sum, most cities had their model coefficients close to the overall means, but there were a few exceptions with values that are extremely lower or higher than the overall mean. Note that shrinkage effect of a hierarchical model automatically corrects the multiple comparison problem (Gelman et al., 2012).

The goodness of fit also varied among the cities (Fig. 5). The highest R^2 (0.93) was found for Sao Paulo and the lowest (0.23) for Aswan. The hockey-stick model performed reasonably well for most cities, with R^2 falling between 0.70 and 0.90. A few cities had superior fit, with R^2 of >0.90, while a few cities had R^2 of <0.60.

The hyper-parameters produced in our hierarchical model indicated that, for a random city, the relationship between *p*BUA and VANUI could be modeled as:

$$pBUA_i = N(\mu_1, \sigma_1) \cdot I(VANUI_i - N(\mu_2, \sigma_2)) \cdot (VANUI_i - N(\mu_2, \sigma_2)) \quad (6)$$

The parameters μ_1, μ_2, σ_1, and σ_2 are treated as random so that they also follow certain distributions (Fig. 6), which indicates their uncertainty. An advantage of Bayesian modeling is that it can use these distributions as new priors for future modeling to fully account for the uncertainties at different levels. The mean values of 0.658, −1.920, 0.318, and 0.769 for μ_1, μ_2, σ_1, and σ_2, respectively, can be used if one wants to treat them as fixed parameters as an frequentist.

3.2. The Influences of urban settings

We used post-model analysis to investigate the potential regulators of city-level settings on the *p*BUA-VANUI relationships. There were no highly correlated linear regulators for the slope coefficients δ (Fig. 7). Population, GDPpc, and openness explained a small variation of δ (r^2 = 0.06, 0.05, and 0.05, respectively) (note that we use r^2 to differ from the R^2 of the hockey-stick models). If the two cities with the highest δ (i.e., outliers) were excluded, population, GDPpc, and openness explained more variation of δ (r^2 = 0.12, 0.06, and 0.10, respectively), but still a small proportion. Other variables were not statistically significantly correlated with δ. We found that population, GDPpc, and precipitation can linearly explain a small proportion of the ϕ variation (r^2 = 0.11, 0.09, and 0.09, respectively) (Fig. 8). The goodness of fit (R^2) of hockey-stick models, however, was correlated with many factors (Fig. 9). Total BUA, BUA density, proximity, cohesion were all significantly correlated with R^2, but explained a small part of the total variation (Fig. 9). Remarkably, cohesion and openness alone can each explain >20% of the total variation in R^2 among the 120 cities (Fig. 9).

The resulting random forests models, which include potential linear and non-linear effects, explained ~7.7% of the variance for the slope δ, ~32.7% for the VANUI threshold (ϕ), and 29.9% for the goodness of fit (R^2). The city-specific setting variables played different roles in predicting our hockey-stick model's coefficients and R^2. Openness, proximity, and cohesion remained the most significant variables in predicting R^2 (Fig. 10). Population, GDPpc, and precipitation were still the most important variables in predicting the VANUI threshold (ϕ) (Fig. 10), which were consistent with those based on linear regression analysis. Population remained the most important variable in predicting the change in δ, which was the same to the linear regression analysis (Fig. 10). Other variables, including GDPpc, openness, and precipitation, appeared marginally important, but it is difficult to quantify which one has the more important influence according to decreases on both accuracy and Gini (Fig. 10). Overall, the variation in coefficients and goodness of fit of the 120 hockey-stick models were not well explained by any particular city-level predictors, linearly and nonlinearly.

3.3. Accuracy of the models

The cross-validated RMSE values were the same (0.126) for the hierarchical model and the no-pooling model, but significantly lower than that of the complete-pooling model (0.152), demonstrating an improved prediction accuracy of 17% (Table 2). For sub-datasets of China

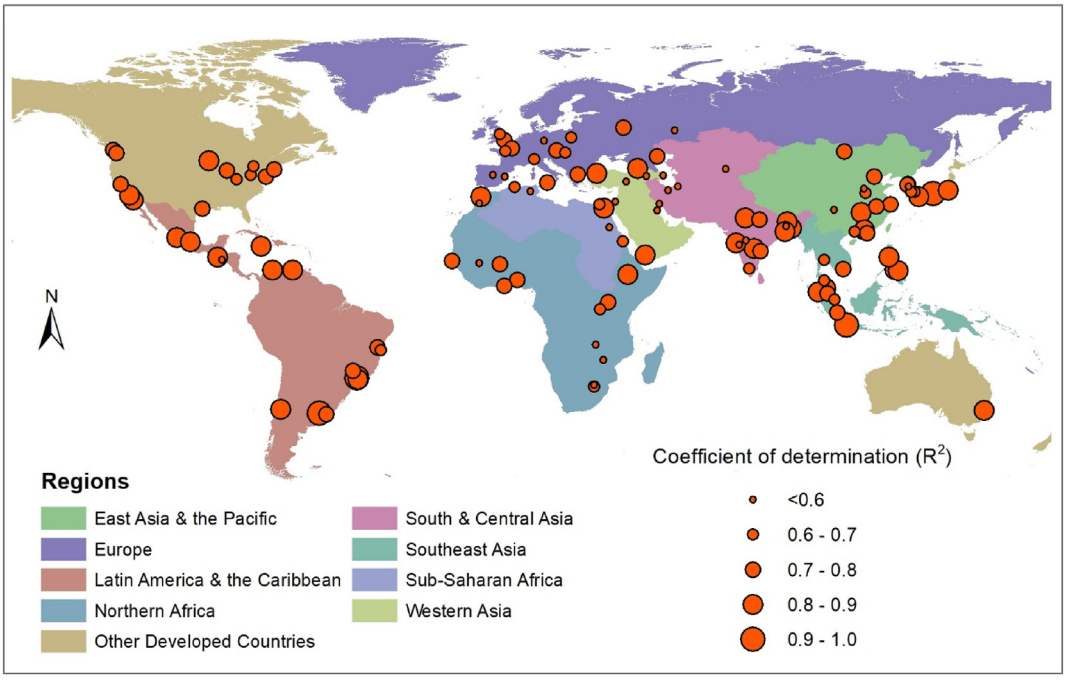

Fig. 5. The variation of the hockey-stick model performance among 120 global cities. The coefficient of determination (R^2) was used as quantitative criteria. Note that regions are defined by grouping countries and Russia is classified as a European country.

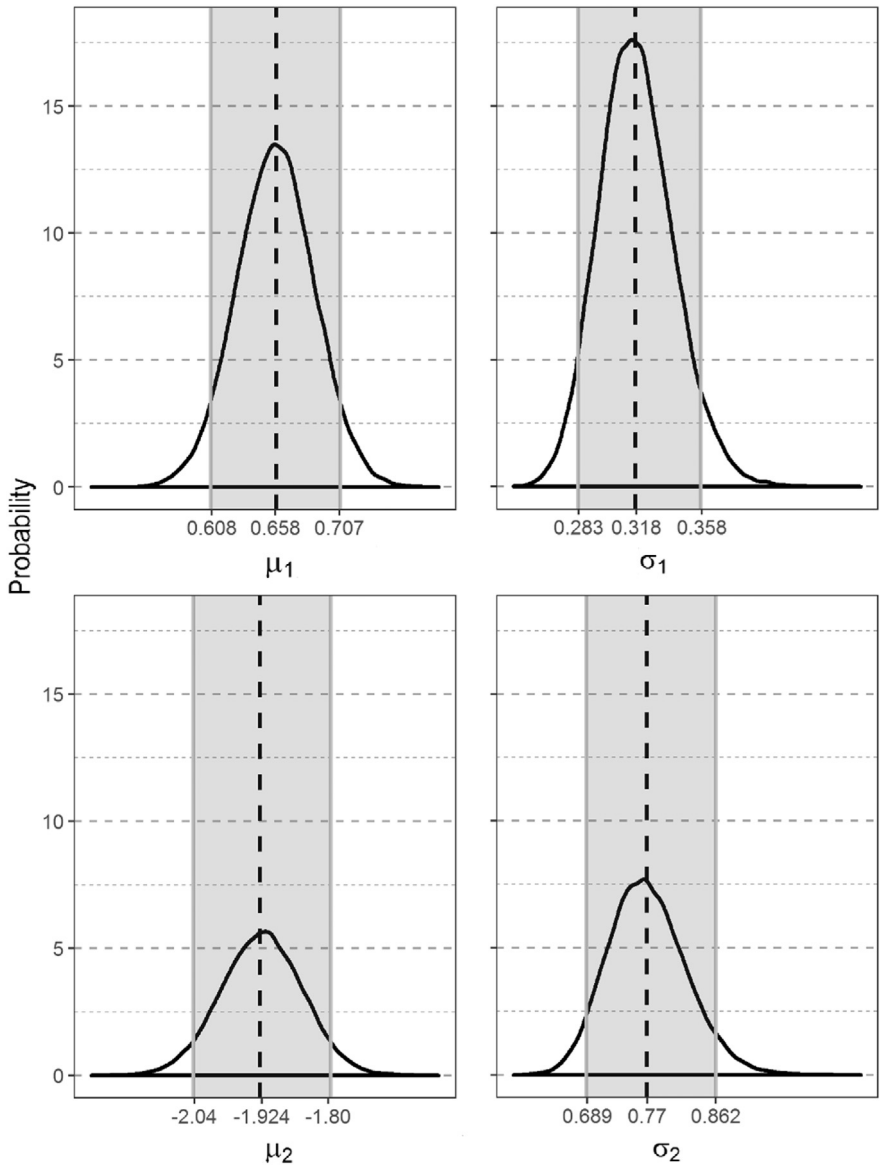

Fig. 6. The posterior distributions of model hyper parameters based on MCMC (100,000 sampling with 50,000 warming up). The black dashed-lines show the mean values; the shaded areas show the 90% credible intervals. μ_1 is the mean slope for the second segment of the hockey-stick model for all cities; and μ_2 is the mean threshold VANUI for the hockey-stick model for all cities. σ_1 and σ_2 are the standard deviations of μ_1 and μ_2.

and the United States, WAIC from the hierarchical model and the no-pooling model was also significantly lower (i.e., higher accuracy) than those of the complete-pooling models (Table 2). While the WAIC was similar between the hierarchical model and the no-pooling model, BHM achieved slightly lower values when the sample size was small (Table 2).

4. Discussion

4.1. Variation of pBUA-VANUI relationships

The *p*BUA-VANUI relationships varied greatly among globally distributed cities (Figs. 4, 5, and 6), suggesting that global and regional delineations of *p*BUA using NTL need to be city-specific. The empirical coefficients from the same hockey-stick model were statistically different among most cities, indicating that pixels from different cities could not be regarded as exchangeable. The overall advantage of a universal model is that it can be readily applied for all cities. Its disadvantage meanwhile is a lowered local accuracy that may arise from unique settings (e.g., covariates that affect the *p*BUA-VANUI relationships) of a local city (Table 2). Supposed that we had used the mean slope (i.e., 0.658) to estimate the *p*BUA in Zhengzhou, China, and Mexico City, Mexico with VANUI >−1.92, the *p*BUA of these pixels in Zhengzhou would be greatly overestimated (by ~180%) while in Mexico they would be underestimated (by ~32%). Consequently, while previous studies (Elvidge et al., 2007; Guo et al., 2017, 2015; Lu and Weng, 2006) achieved good results of regional/global mapping of BUA or impervious area from NTL data by using a universal model trained from pooled samples, there is still room to improve both the overall and local accuracy by applying BHM. Our results showed that it may increase up to 17% in terms of RMSE globally by considering the unique *p*BUA-VAUNI relationship for each city.

The variation of *p*BUA-VANUI relationships among cities, however, is not well regulated by any city-level variables (Figs. 7–9). This implies that there are apparent variations that we already know of, but that we cannot predict. The population size can explain a small proportion of δ and ϕ with a lognormal regression (6% and 11%, respectively). A larger population is associated with a larger slope, suggesting cities with a larger population size tend to expand more BUA for the same amount increase of VANUI. This is in consistence with the additive and

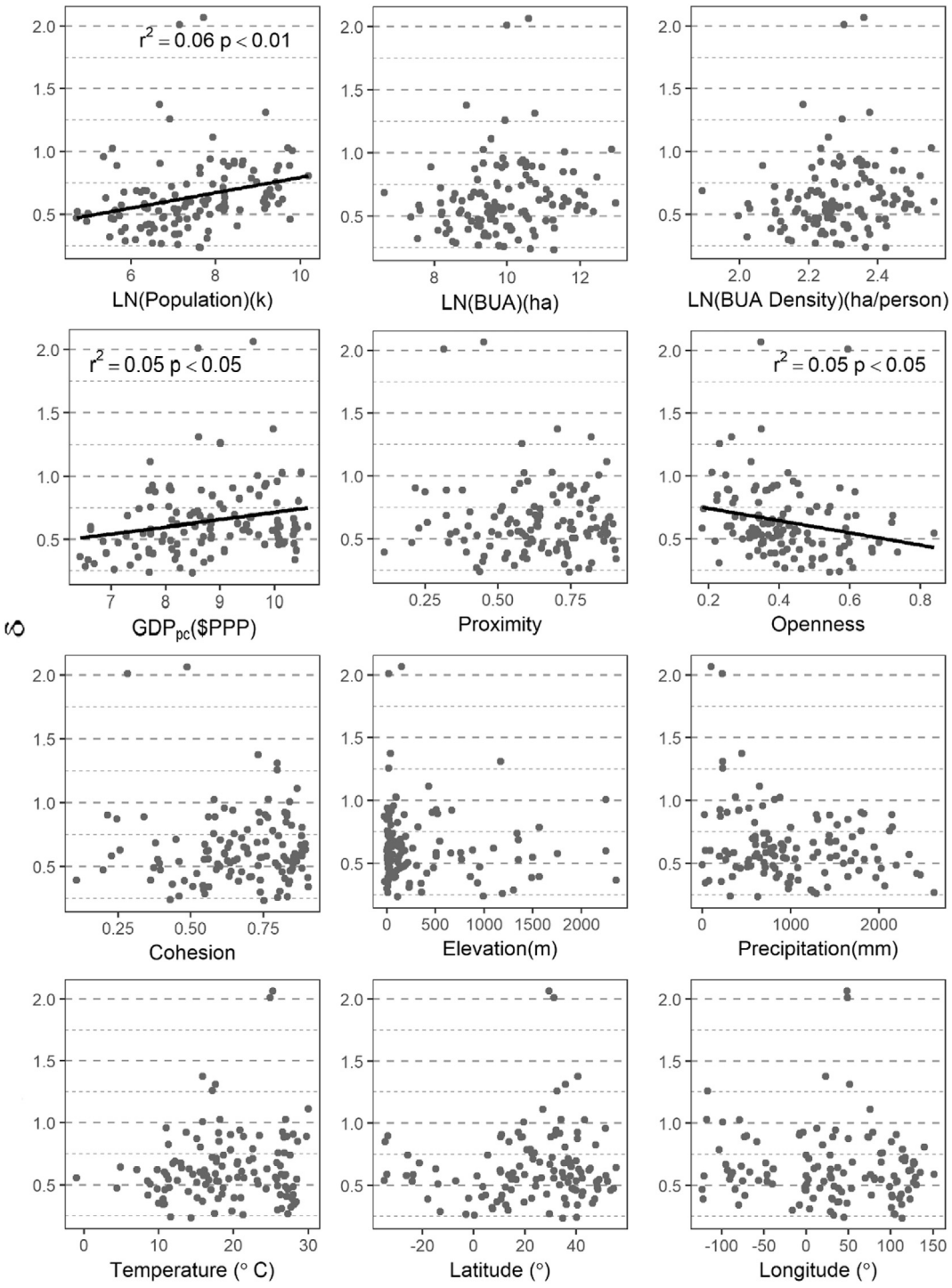

Fig. 7. The linear or log-linear regression relationships between the model coefficient slope (δ) and the socioeconomic, climatic, geographic, and landscape structure variables based on 120 random cities.

positive effects of population to the *p*BUA-NTL relationship (Elvidge et al., 2007). Cities with a larger population also tend to have a larger threshold VANUI value, which is also reflected in the logistic relationship between optical threshold NTL DN value and the size of urban clusters (Zhou et al., 2014). However, such effects may disappear when population reaches certain threshold (i.e., a lognormal or logistic relationship) because NTL would become saturated due to its internal limitation (Bennett and Smith, 2017). GDPpc has small but similar effects on both coefficients as total population. Higher GDPpc may imply a higher total energy/light consumption of a city as a whole, which in turn will lead to more light blooming and thus a larger threshold VANUI value. Meanwhile, higher GDPpc may also mean higher economic productivity of the urban land, thus lowering the increasing rate of *p*BUA with NTL. The rate of BUA expansion decreased as a city's GDPpc increased (Seto et al., 2011). This effect of GDPpc again would finally disappear because of the saturation of the NTL signal. In sum, it remains difficult to explain why a city with more rainfall would result in a lower VANUI threshold. One possible reason would be that the image quality is affected by the clouds (e.g., moonlit clouds may not be completely excluded, thereby causing an overall decline of NTL brightness) (Elvidge et al., 2001, 1997).

The landscape structure did not affect both δ and ϕ, except that openness may be weakly correlated with the slope coefficient (δ). A

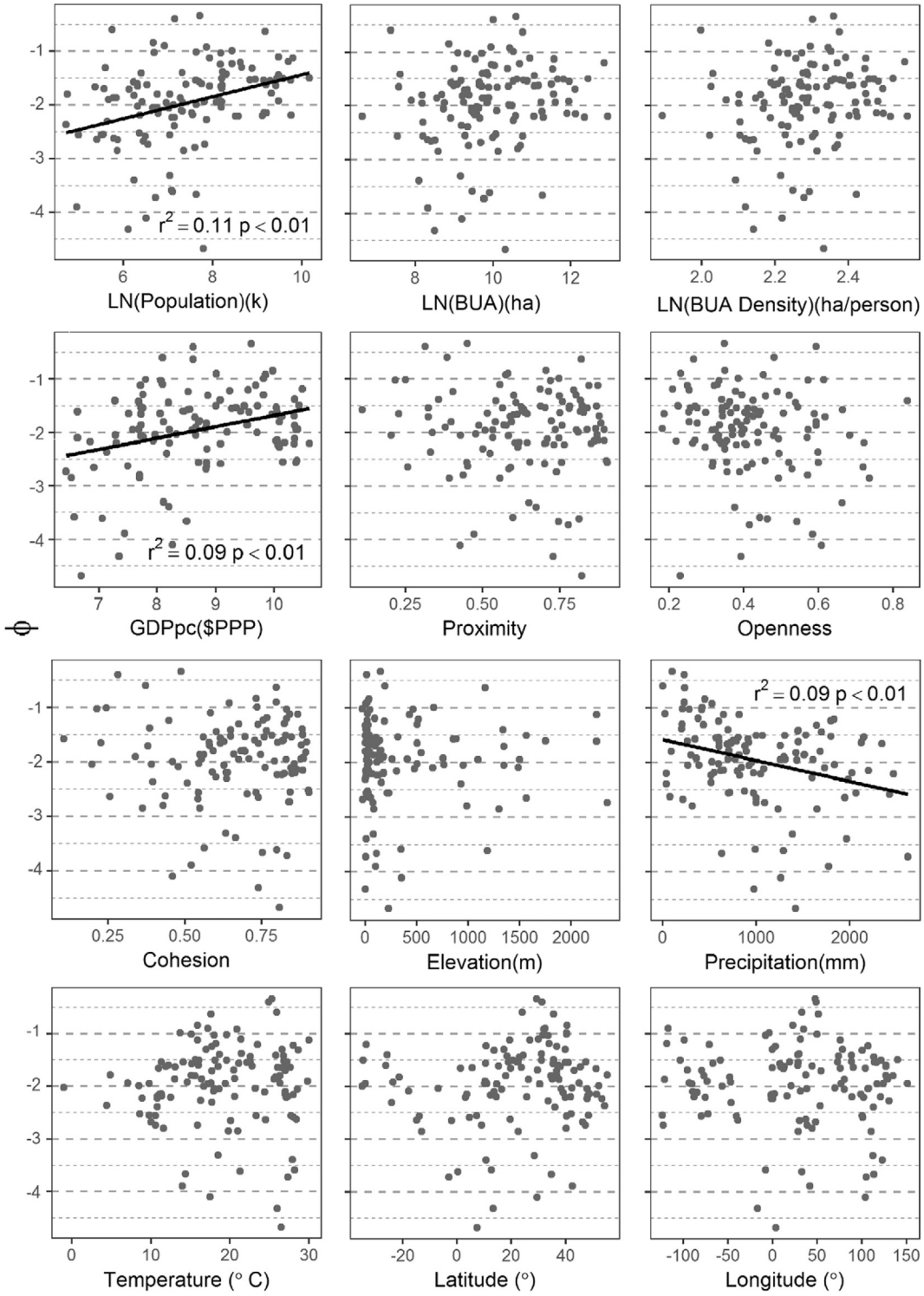

Fig. 8. The linear or log-linear regression relationship between the model coefficient breakpoint (ϕ) and socioeconomic, climatic, geographic, and landscape structure variables based on 120 random cities.

larger openness value means on average more open space within a half-kilometer radius, which allows more light to scatter and illuminate non-BUA space, and thus can lower the increasing rate of *p*BUA with VANUI. The goodness of fit (R^2) of the hockey-stick model for the 120 cities, however, is correlated with the landscape metrics. The positive correlation between R^2 and cohesion/proximity, and the negative correlation between R^2 and openness suggests that cities with more compacted and continuous BUA (e.g., many large cities in high-income regions) can be predicted with higher confidence than others. Openness as a measure of fragmentation is scale-dependent. If the data resolution was improved, openness computed based on a smaller circle would be reduced for BUA pixels. Therefore, new generation NTL data with finer spatial resolution (e.g., VIIRS-DNB) is critical to increase the performance of BUA mapping (Elvidge et al., 2013). The random forests

model, which considers both linear and non-linear effects, explained 7.7% of the variation of δ (note: slope is the most important model coefficient for mapping BUA), 32.7% of the variation of ϕ, and 29.9% of R^2. The most significant variables that appeared in random forests, were also consistent with those based on linear regression analysis, including population and GDPpc for both δ and ϕ, openness for δ, precipitation for ϕ, and openness, cohesion, and proximity for R^2.

In summary, the variation of the hockey-stick model's performance can be partially attributed to landscape metrics, and that of the model coefficients can be partially attributed to socioeconomic variables, while climatic and geographic variables have little effects on both. However, we are still uncertain about what major driving forces are responsible for the variation among these coefficients and model performances. Future studies should be devoted to continuously exploring the variation of model coefficients and performance among cities in improving BUA mapping form NTL.

4.2. Why hierarchical models?

The advantage of hierarchical models over complete-pooling models is obvious when group characteristics (i.e., cities) are different in certain ways to make individuals (i.e., pixels) not interchangeable among

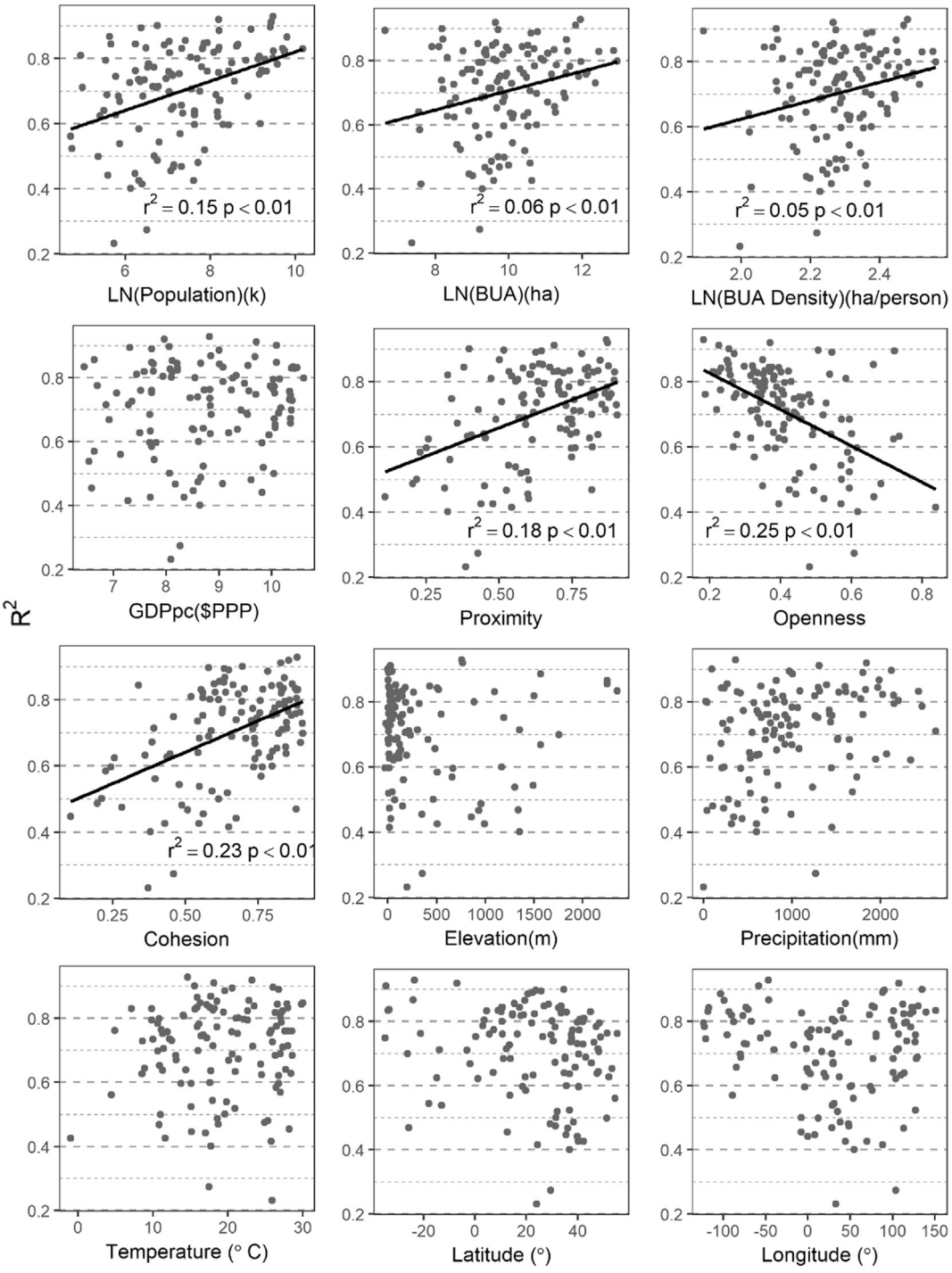

Fig. 9. The linear or log-linear regression relationship between the model goodness of fit (R^2) and socioeconomic, climatic, geographic, and landscape structure variables based on 120 random cities.

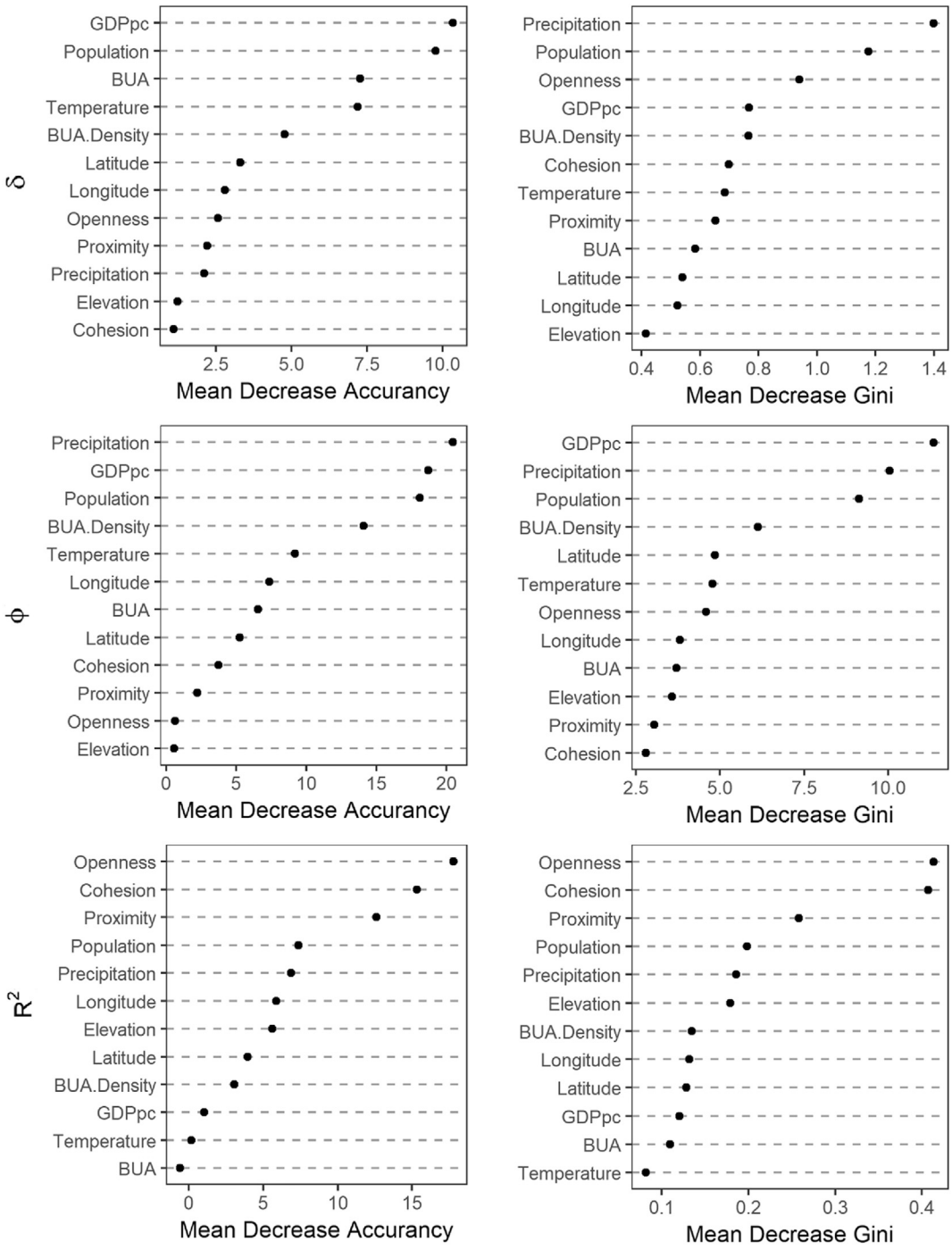

Fig. 10. Relative importance of the 12 variables (Table 1) in predicting *p*BUA revealed by random forests (1000 trees) for the slope (δ), the VANUI threshold (ϕ), and the goodness of fit (R^2). The importance of a variable was measured by mean decrease in accuracy and Gini.

groups, as they can significantly improve prediction accuracy compared to the complete-pooling models (Table 2).

The advantages of hierarchical models over no-pooling models are not so obvious because they demonstrated similar prediction accuracy, especially when the sample size is large (Table 2), but there are a few implicit benefits from the hierarchical modeling. Firstly, both no-pooling and complete-pooling models can be regarded as a special case of a hierarchical model. When there is little group-level variation, the hierarchical model reduces to the classical complete-pooling model with no group indicators. Conversely, when there is a great group-level variation, the hierarchical model reduces to the classical no-pooling model with group indicators (Gelman and Hill, 2007).

Table 2
Prediction accuracy based on the root mean square error (RMSE) and the Watanabe-Akaike Information Criterion (WAIC) among the Bayesian Hierarchical Model (BHM), the Bayesian no-pooling model, and the Bayesian complete-pooling model.

Criteria	BHM	No-pooling	Pooling	Region	Group size	Data size
RMSE	0.126	0.126	0.152	Globe	120 cities	541,696 pixels
WAIC	−18,671.1	−18,669.8	−6131.4	China	10 cities	6406 pixels
WAIC	−569.3	−562.0	−367.3.3	China	10 cities	500 pixels
WAIC	−8891.0	−8890.3	−6131.6	U.S.	10 cities	8000 pixels
WAIC	−498.5	−477.4	−362.2	U.S.	10 cities	500 pixels

Mathematically, one can force a hierarchical model to become a no-pooling model or complete-pooling model by setting hierarchical variance parameters to zero or infinity (in our case, σ_0, σ_1, and σ_2). This suggests that even when we do not gain any additional benefits from the hierarchical model, there is little risk of using the hierarchical model (at worst it is the same as the no-pooling/complete-pooling model). Therefore, hierarchical models are more plausible because they guarantee the best prediction accuracy regardless of how significant group-level variations are. More importantly, one can get the most benefits from hierarchical models when groups are different but not completely different (Gelman and Hill, 2007). Secondly, hierarchical models can achieve higher prediction accuracies than no-pooling models, although it depends on sample size. From a Bayesian's perspective, the hyper model (i.e., Eq. (6)) provides an informative prior for each city-specific model. When the sample size in a city is large, there is strong information included in that city's data so there is no necessity to use information from the prior (Bayes' rule suggests that in such cases, the posterior is close to the likelihood). However, when sample size is small, this prior information becomes very useful as it regulates the modeler to reduce over-fitting (by telling the modeler a reasonable range of the parameters). We demonstrated this by reducing the sample to 50 pixels per city (which is not small compared to many observational studies in Ecology and Geography) to show increased prediction accuracy of BHM over no-pooling models. In reality, we often have a very limited sample for one or a few groups. Previous studies have demonstrated that when there are groups with limited samples, hierarchical models have the ability to increase overall prediction accuracy and reduce uncertainty (Alberti, 2005; Qian et al., 2015a, 2015b). Lastly and most importantly, the estimated hyper distribution of parameters (Eq. (6)) is valuable for future (and group-specific) models under a Bayesian framework. Often, one usually has a new but small sample for future modeling. In such cases, a new Bayesian model using Eq. (6) as a prior with new data derived likelihoods can gradually update the *p*BUA-VANUI function so that it can best fit city-specific/region-specific data. Even with very limited new data, including Eq. (6) as a prior can guarantee that the new model will be properly regulated. Alternatively, with an informative prior it can reduce the need of large samples, saving costs of both human and financial resources. Eq. (6) can also be used as a useful prior for mapping BUA using VANUI for a new region and for a different year.

4.3. Broad implications

We focused on BUA mapping from VANUI that is derived from DMSP-OLS NTL and MODIS NDVI product. Our methods, in principle, apply to other similar NTL derived indices for both impervious surface area and BUA mapping, and more widely to the applications of mapping other biophysical quantities from remote sensing. The application of remote sensing in mapping land surface properties often relies on regression models between the phenomenon of interest and remote sensing data. Yet this same regression model can vary among different spatial or temporal units (e.g., ecoregion, administrative unit, size, year, etc.) due to heterogeneity caused by spatial, temporal, or other organizational factors. For example, the same form of a vegetation photosynthesis model could be applied in various ecosystems, but specific parameters should be tuned differently in different ecosystem types or in different regions of the same ecosystem type (Wang et al., 2010; Xiao et al., 2005, 2004). The same regression model between LiDAR derived variables and aboveground biomass (AGB) may be used for AGB mapping, but it may vary by forest age groups and forest type groups (Boudreau et al., 2008; Giannico et al., 2016). To map soil salinity, the same regression relationship between soil salinity and hyper-spectral reflectance may vary in specific coefficients among different plant communities (Zhang et al., 2011). Following this school of thought, there might always be room to improve the overall accuracy by considering the different responses of ecosystem functions to the same set of predictors. This could be realized by grouping on certain characteristics of the subject to reduce the effects of confounding factors (by making them similar among units within a group) to the same relationship of interest among groups. A hierarchical model, or a no-pooling model with group indicators, can thus be conducted for improved mapping accuracy. However, considering the many advantages discussed above, we strongly recommend Bayesian hierarchical models.

5. Conclusions

We developed a Bayesian hierarchical hockey-stick model to investigate the variations of the *p*BUA-VANUI relationship among 120 cities across the globe. We found that there were substantial differences in the model parameters (i.e., the slope (0.658 ± 0.318)) and the threshold VANUI (-1.92 ± 0.769, log scale) and model performance (i.e., the coefficients of determination (0.71 ± 0.14)) among these cities. However, only a small proportion of the substantial variation in model parameters can be attributed to socioeconomic differences (e.g., population, economy, and city size) and a small proportion of the variation in model performance can be explained by landscape structures and socioeconomic measures (e.g., compactness, fragmentation, and population). By comparing Bayesian hierarchical models (BHMs) to the no-pooling and complete-pooling models, we found that BHMs and the no-pooling models significantly increased prediction accuracy of *p*BUA over the complete-pooling models that ignore the among-city variations. Both BHMs and no-pooling models outperformed complete-pooling models by a ~17% increase in prediction accuracy for the 120 globally distributed cities through considering the unique *p*BUA-VANUI relationship by city. Additionally, the BHMs performed better than no-pooling models in providing meaningful priors for future Bayesian modeling and in improving prediction accuracy when sample size is limited. Since regression approaches are often applied in remote sensing science and the hierarchical structure commonly exists in landscapes due to scale-dependent heterogeneity, the hierarchical approaches developed in this study can be adopted and extended to map other land surface properties for improved accuracy as well.

Acknowledgments

We would like to acknowledge the financial support from the Land Cover and Land Use Change Program (LCLUC) of the National Aeronautics and Space Administration (NASA) through its grant to Michigan State University (Grant No. NNX15AD51G), and the financial support from the "Dynamics of Coupled Natural and Human Systems (CNH)" Program of the NSF (#1313761). We also thank Connor Crank for proofreading our manuscript.

References

Alberti, M., 2005. The effects of urban patterns on ecosystem function. Int. Reg. Sci. Rev. 28, 168–192. https://doi.org/10.1177/0160017605275160.

Angel, S., Sheppard, S.C., Civco, D.L., Buckley, R., Chabaeva, A., Gitlin, L., Kraley, A., Parent, J., Perlin, M., 2005. The Dynamics of Global Urban Expansion. 1. Transp. Urban Dev. Dep. World Bank, p. 3. https://doi.org/10.1038/nature09440.

Angel, S., Parent, J., Civco, D.L., Blei, A.M., 2016. Atlas of Urban Expansion - The 2016 Edition, Volume 1: Areas and Densities. Choice Reviews Online https://doi.org/10.5860/CHOICE.50-1227.

Bennett, M.M., Smith, L.C., 2017. Advances in using multitemporal night-time lights satellite imagery to detect, estimate, and monitor socioeconomic dynamics. Remote Sens. Environ. https://doi.org/10.1016/j.rse.2017.01.005.

Bento, A.P., Gaulton, A., Hersey, A., Bellis, L.J., Chambers, J., Davies, M., Kruger, F.A., Light, Y., Mak, L., McGlinchey, S., Nowotka, M., Papadatos, G., Santos, R., Overington, J.P., Bredel, M., Jacoby, E., Breiman, L., Fourches, D., Muratov, E., Tropsha, A., Freyhult, E., Prusis, P., Lapinsh, M., Wikberg, J.E., Moulton, V., Gustafsson, M.G., Gaulton, A., Bellis, L.J., Bento, A.P., Chambers, J., Davies, M., Hersey, A., Light, Y., McGlinchey, S., Michalovich, D., Al-Lazikani, B., Overington, J.P., Kooistra, A.J., Kuhne, S., de Esch, I.J.P., Leurs, R., de Graaf, C., Paricharak, S., Cortés-Ciriano, I., Ijzerman, A.P., Malliavin, T.E., Bender, A., Rezácová, P., Borek, D., Moy, S.F., Joachimiak, A., Otwinowski, Z., Strobl, C., Boulesteix, A.-L., Zeileis, A., Hothorn, T., Van Westen, G.J.P., Van Den Hoven, O.O., Van Der Pijl, R., Mulder-Krieger, T., De Vries, H., Wegner, J.K., Ijzerman, A.P., van Vlijmen, H.W.T., Bender, A., Swier, R.F., Wegner, J.K., Ijzerman, A.P., van Vlijmen, H.W.T., Bender, A.,

Liaw, A., Wiener, M., Jorgensen, W.L., Friedman, J.H., Van Westen, G.J.P., Wegner, J.K., Geluykens, P., Kwanten, L., Vereycken, I., Peeters, A., Ijzerman, A.P., van Vlijmen, H.W.T., Bender, A., Breitenbach, M., Nielsen, R., Grudic, G.Z., Meinshausen, N., Hatko, S., 2013. Classification and regression by randomForest. Nucleic Acids Res. 5, 983–999. https://doi.org/10.1023/A:1010933404324.

Boudreau, J., Nelson, R.F., Margolis, H.A., Beaudoin, A., Guindon, L., Kimes, D.S., 2008. Regional aboveground forest biomass using airborne and spaceborne LiDAR in Québec. Remote Sens. Environ. 112, 3876–3890. https://doi.org/10.1016/j.rse.2008.06.003.

Burchfield, M., Overman, H.G., Puga, D., Turner, M.A., 2006. Causes of sprawl: a portrait from space. Q. J. Econ. 121, 587–633. https://doi.org/10.1162/qjec.2006.121.2.587.

Cao, X., Chen, J., Imura, H., Higashi, O., 2009. A SVM-based method to extract urban areas from DMSP-OLS and SPOT VGT data. Remote Sens. Environ. 113, 2205–2209. https://doi.org/10.1016/j.rse.2009.06.001.

Chen, J., Zhu, L., Fan, P., Tian, L., Lafortezza, R., 2016. Do green spaces affect the spatiotemporal changes of $PM_{2.5}$ in Nanjing? Ecol. Process. 5. https://doi.org/10.1186/s13717-016-0052-6.

Cleveland, W.S., 1993. Visualizing Data. Hobart Press, Summit, NJ.

Elvidge, C.D., Baugh, K.E., Kihn, E.A., Kroehl, H.W., Davis, E.R., 1997. Mapping city lights with nighttime data from the DMSP operational linescan system. Photogramm. Eng. Remote. Sens. 63, 727–734.

Elvidge, C.D., Imhoff, M.L., Baugh, K.E., Hobson, V.R., Nelson, I., Safran, J., Dietz, J.B., Tuttle, B.T., 2001. Night-time lights of the world: 1994–1995. ISPRS J. Photogramm. Remote Sens. 56, 81–99. https://doi.org/10.1016/S0924-2716(01)00040-5.

Elvidge, C.D., Tuttle, B.T., Sutton, P.C., Baugh, K.E., Howard, A.T., Milesi, C., Bhaduri, B., Nemani, R., 2007. Global distribution and density of constructed impervious surfaces. Sensors 7, 1962–1979. https://doi.org/10.3390/s7091962.

Elvidge, C.D., Baugh, K.E., Zhizhin, M., Hsu, F.-C., 2013. Why VIIRS data are superior to DMSP for mapping nighttime lights. Proc. Asia-Pacific Adv. Netw. 35, 62. https://doi.org/10.7125/APAN.35.7.

Estoque, R.C., Murayama, Y., Myint, S.W., 2017. Effects of landscape composition and pattern on land surface temperature: an urban heat island study in the megacities of Southeast Asia. Sci. Total Environ. 577, 349–359. https://doi.org/10.1016/J.SCITOTENV.2016.10.195.

Fan, P., Xu, L., Yue, W., Chen, J., 2017. Accessibility of public urban green space in an urban periphery: the case of Shanghai. Landsc. Urban Plan. 165, 177–192. https://doi.org/10.1016/J.LANDURBPLAN.2016.11.007.

Gao, B., Huang, Q., He, C., Ma, Q., 2015. Dynamics of Urbanization Levels in China from 1992 to 2012: perspective from DMSP/OLS Nighttime Light Data. Remote Sens. 7 (2), 1721–1735.

Gelman, A., Hill, J., 2007. Data Analysis Using Regression and Multilevel/Hierarchical Models. Cambridge https://doi.org/10.2277/0521867061.

Gelman, A., Rubin, D.B., 1992. Inference from iterative simulation using multiple sequences. Stat. Sci. 7, 457–472. https://doi.org/10.1214/ss/1177011136.

Gelman, A., Hill, J., Yajima, M., 2012. Why we (usually) don't have to worry about multiple comparisons. J. Res. Educ. Effect. 5, 189–211. https://doi.org/10.1080/19345747.2011.618213.

Gelman, A., Hwang, J., Vehtari, A., 2014. Understanding predictive information criteria for Bayesian models. Stat. Comput. 24, 997–1016. https://doi.org/10.1007/s11222-013-9416-2.

Giannico, V., Lafortezza, R., John, R., Sanesi, G., Pesola, L., Chen, J., 2016. Estimating stand volume and above-ground biomass of urban forests using LiDAR. Remote Sens. 8. https://doi.org/10.3390/rs8040339.

Guo, W., Lu, D., Wu, Y., Zhang, J., 2015. Mapping impervious surface distribution with integration of SNNP VIIRS-DNB and MODIS NDVI Data. Remote Sens. 7, 12459–12477. https://doi.org/10.3390/rs70912459.

Guo, W., Lu, D., Kuang, W., 2017. Improving fractional impervious surface mapping performance through combination of DMSP-OLS and MODIS NDVI data. Remote Sens. 9. https://doi.org/10.3390/rs9040375.

Kyba, C., Garz, S., Kuechly, H., de Miguel, A., Zamorano, J., Fischer, J., Hölker, F., 2014. High-resolution imagery of Earth at night: new sources, opportunities and challenges. Remote Sens. 7, 1–23. https://doi.org/10.3390/rs70100001.

Li, X., Zhou, Y., 2017. Urban mapping using DMSP/OLS stable night-time light: a review. Int. J. Remote Sens. 38, 6030–6046. https://doi.org/10.1080/01431161.2016.1274451.

Liu, L., Leung, Y., 2015. A study of urban expansion of prefectural-level cities in South China using night-time light images. Int. J. Remote Sens. 36, 5557–5575. https://doi.org/10.1080/01431161.2015.1101650.

Lu, D., Weng, Q., 2006. Use of impervious surface in urban land-use classification. Remote Sens. Environ. 102, 146–160. https://doi.org/10.1016/j.rse.2006.02.010.

Mertes, C.M., Schneider, A., Sulla-Menashe, D., Tatem, A.J., Tan, B., 2015. Detecting change in urban areas at continental scales with MODIS data. Remote Sens. Environ. 158, 331–347. https://doi.org/10.1016/j.rse.2014.09.023.

Nassauer, J.I., Wu, J.G., Xiang, W.-N., 2014. Actionable urban ecology in China and the world: integrating ecology and planning for sustainable cities. Landsc. Urban Plan. 125, 207–208. https://doi.org/10.1016/J.LANDURBPLAN.2014.02.022.

Park, H., Fan, P., John, R., Chen, J., 2017. Urbanization on the Mongolian Plateau after economic reform: changes and causes. Appl. Geogr. 86, 118–127. https://doi.org/10.1016/J.APGEOG.2017.06.026.

Pesaresi, M., Huadong, G., Blaes, X., Ehrlich, D., Ferri, S., Gueguen, L., Halkia, M., Kauffmann, M., Kemper, T., Lu, L., Marin-Herrera, M.A., Ouzounis, G.K., Scavazzon, M., Soille, P., Syrris, V., Zanchetta, L., 2013. A global human settlement layer from optical HR/VHR RS data: concept and first results. IEEE J. Sel. Top. Appl. Earth Obs. Remote Sens. 6, 2102–2131. https://doi.org/10.1109/JSTARS.2013.2271445.

Qian, S.S., 2014. Ecological threshold and environmental management: a note on statistical methods for detecting thresholds. Ecol. Indic. 38, 192–197. https://doi.org/10.1016/j.ecolind.2013.11.008.

Qian, S.S., 2016. Environmental and Ecological Statistics With R. Chapman and Hall/CRC, London, New York.

Qian, S., Cuffney, T., Alameddine, I., 2010. On the application of multilevel modeling in environmental and ecological studies. Ecology 91, 355–361. https://doi.org/10.1890/09-1043.1.

Qian, S.S., Chaffin, J.D., Dufour, M.R., Sherman, J.J., Golnick, P.C., Collier, C.D., Nummer, S.A., Margida, M.G., 2015a. Quantifying and reducing uncertainty in estimated microcystin concentrations from the ELISA method. Environ. Sci. Technol. 49, 14221–14229. https://doi.org/10.1021/acs.est.5b03029.

Qian, S.S., Stow, C.A., Cha, Y., 2015b. Implications of steins paradox for environmental standard compliance assessment. Environ. Sci. Technol. 49, 5913–5920. https://doi.org/10.1021/acs.est.5b00656.

Seto, K.C., Fragkias, M., Güneralp, B., Reilly, M.K., 2011. A meta-analysis of global urban land expansion. PLoS One 6. https://doi.org/10.1371/journal.pone.0023777.

Shelton, A.O., Dick, E.J., Pearson, D.E., Ralston, S., Mangel, M., Walters, C., 2012. Estimating species composition and quantifying uncertainty in multispecies fisheries: hierarchical Bayesian models for stratified sampling protocols with missing data. Can. J. Fish. Aquat. Sci. 69, 231–246. https://doi.org/10.1139/f2011-152.

Wang, Z., Xiao, X., Yan, X., 2010. Modeling gross primary production of maize cropland and degraded grassland in northeastern China. Agric. For. Meteorol. 150, 1160–1167. https://doi.org/10.1016/j.agrformet.2010.04.015.

Watanabe, S., 2010. Asymptotic equivalence of Bayes cross validation and widely applicable information criterion in singular learning theory. J. Mach. Learn. Res. 11, 3571–3594.

Wu, J., 2014. Urban ecology and sustainability: the state-of-the-science and future directions. Landsc. Urban Plan. 125, 209–221. https://doi.org/10.1016/j.landurbplan.2014.01.018.

Xiao, X., Zhang, Q., Braswell, B., Urbanski, S., Boles, S., Wofsy, S., Moore, B., Ojima, D., 2004. Modeling gross primary production of temperate deciduous broadleaf forest using satellite images and climate data. Remote Sens. Environ. 91, 256–270. https://doi.org/10.1016/j.rse.2004.03.010.

Xiao, X., Zhang, Q., Saleska, S., Hutyra, L., De Camargo, P., Wofsy, S., Frolking, S., Boles, S., Keller, M., Moore, B., 2005. Satellite-based modeling of gross primary production in a seasonally moist tropical evergreen forest. Remote Sens. Environ. 94, 105–122. https://doi.org/10.1016/j.rse.2004.08.015.

Xiao, P., Wang, X., Feng, X., Zhang, X., Yang, Y., 2014. Detecting China's urban expansion over the past three decades using nighttime light data. IEEE J. Sel. Top. Appl. Earth Obs. Remote Sens. 7, 4095–4106. https://doi.org/10.1109/JSTARS.2014.2302855.

Yun, J., Qian, S.S., 2015. A hierarchical model for estimating long-term trend of atrazine concentration in the surface water of the contiguous U.S. J. Am. Water Resour. Assoc. 51, 1128–1137. https://doi.org/10.1111/jawr.12284.

Zhang, Q., Seto, K.C., 2011. Mapping urbanization dynamics at regional and global scales using multi-temporal DMSP/OLS nighttime light data. Remote Sens. Environ. 115, 2320–2329. https://doi.org/10.1016/j.rse.2011.04.032.

Zhang, T.T., Zeng, S.L., Gao, Y., Ouyang, Z.T., Li, B., Fang, C.M., Zhao, B., 2011. Using hyperspectral vegetation indices as a proxy to monitor soil salinity. Ecol. Indic. 11, 1552–1562. https://doi.org/10.1016/j.ecolind.2011.03.025.

Zhang, Q., Schaaf, C., Seto, K.C., 2013. The vegetation adjusted NTL urban index: a new approach to reduce saturation and increase variation in nighttime luminosity. Remote Sens. Environ. 129, 32–41. https://doi.org/10.1016/j.rse.2012.10.022.

Zhou, Y., Smith, S.J., Elvidge, C.D., Zhao, K., Thomson, A., Imhoff, M., 2014. A cluster-based method to map urban area from DMSP/OLS nightlights. Remote Sens. Environ. 147, 173–185. https://doi.org/10.1016/j.rse.2014.03.004.

Zhou, N., Hubacek, K., Roberts, M., 2015a. Analysis of spatial patterns of urban growth across South Asia using DMSP-OLS nighttime lights data. Appl. Geogr. 63, 292–303.

Zhou, Y., Smith, S.J., Zhao, K., Imhoff, M., Thomson, A., Bond-Lamberty, B., Asrar, G.R., Zhang, X., He, C., Elvidge, C.D., 2015b. A global map of urban extent from nightlights. Environ. Res. Lett. 10, 054011. https://doi.org/10.1088/1748-9326/10/5/054011.

Zhuo, L., Zheng, J., Zhang, X., Li, J., Liu, L., 2015. An improved method of night-time light saturation reduction based on EVI. Int. J. Remote Sens. 36, 4114–4130. https://doi.org/10.1080/01431161.2015.1073861.